

SPACE-CHARGE BEAM PHYSICS RESEARCH AT THE UNIVERSITY OF MARYLAND ELECTRON RING (UMER)*

S. Bernal[†], G. Bai, B. Beaudoin, D. Feldman, R. Feldman, R. Fiorito, T.F. Godlove, I. Haber, R.A. Kishek, C. Papadopoulos, B. Quinn, M. Reiser, D. Stratakis, D. Sutter, K. Tian, T.C.J. Tobin, M. Walter, C. Wu, and P.G. O’Shea, Institute for Research in Electronics and Applied Physics, University of Maryland, College Park, USA

Abstract

The University of Maryland electron ring (UMER) is a low-energy, high current recirculator for beam physics research with relevance to any applications that rely on intense beams of high quality. We review the space-charge physics issues, experimental and computational investigations, which are currently being conducted at the UMER facility. The physics issues cover a broad range, but we focus on transverse beam dynamics: halo formation, strongly asymmetric beams, Montague resonances, equipartitioning, etc. Furthermore, we report on recent developments in experiments, simulations, and improved diagnostics for space-charge dominated beams.

INTRODUCTION

Space charge is an important factor at the source and in the low-energy sections of most electron and hadron accelerators. Space charge can drive emittance growth and halo formation through several mechanisms [1]. It also plays a significant role in the analysis of beam stability and resonances even for emittance-dominated beams, and in the evolution of beam bunches (e.g., energy spread, beam-edge erosion, resistive wall instability, etc). Thus, understanding space charge is paramount for the development of advanced accelerators with relevance to FELs, high-energy density physics, spallation neutron sources, high-energy physics, etc.

The role of space charge in the beam’s transverse transport dynamics can be characterized through an *intensity parameter* χ , defined for the matched beam in an equivalent uniform focusing lattice. The parameter is equal to the ratio of transverse space charge to external focusing forces [2]; χ is equal to zero in the limit of zero current and to 1 in the limit of zero emittance. If the same model is applied to a circular lattice, the space charge tune depression is given by

$$\frac{\nu}{\nu_0} = (1 - \chi)^{1/2}, \quad (1)$$

where ν_0 is the bare tune. The *fractional tune shift*, $\Delta\nu/\nu_0$, is given approximately by $\chi/2$, if $\Delta\nu \ll \nu_0$. Traditionally, the tune shift is chosen to satisfy $\Delta\nu \leq 0.25$ to avoid

* This work is funded by US Dept. of Energy grant numbers DE-FG02-94ER40855 and DE-FG02-92ER54178, and the office of Naval Research grant N00014-02-1-0914.

[†] sabern@umd.edu

integer and half-integer resonances. This “Laslett tune-shift” limit has been exceeded in various experiments. A tune shift of 1.9, the largest measured in a circular machine, was achieved by Maschke in the AGS at Brookhaven National Laboratory in 1977 [3]. Linear accelerators, by contrast, can operate in regimes with χ as high as 0.9. Since “tune” is not defined in this case, however, the effect of space charge is expressed instead by the ratio of betatron wavenumbers with and without space charge: k/k_0 . Thus, linear machines can operate with k/k_0 as low as 0.3.

Unlike the case with most accelerators, space charge is *not* a perturbation in UMER, even when operating in the emittance-dominated regime ($\lesssim 1$ mA at 10 keV). Table 1 summarizes the parameters at four operating beam currents in UMER. At beam currents $\gtrsim 20$ mA, UMER yields unprecedented tune depressions of < 0.3 , or fractional tune shifts $> 70\%$. The beam dynamics in this regime of extreme space charge is dominated by collective effects and is largely unexplored. With UMER, we are addressing physics issues in both transverse and longitudinal beam dynamics: beam injection/matching, emittance growth and halo formation, resonance crossing, anisotropic beams, coupling resonances and emittance exchange and equipartitioning, bunch capture and shaping, etc.

Table 1: Main beam parameters in UMER current experiments (10 keV, $\nu_0 = 7.29$)

Beam Current	Emitt. ¹ (μm)	Beam Rad. (mm)	Tune Dep.
500-700 μA	5.5	1.3-1.4	0.84-0.79
5.8 mA	16	2.9	0.53
23 mA	20	5.0	0.22
100 mA	60	10.3	0.16

¹ 4RMS, unnormalized.

The study of some of these effects in large accelerators is difficult for fundamental or for practical reasons. Synchrotron radiation, for example, may easily mask effects from space charge; in another example, halo studies with high-energy beams may become problematic because of wall activation. Therefore, a low-energy, high-current electron machine represents a cost-effective alternative for beam dynamics studies. Other ion and electron machines for scaled experiments and/or exploration of new technologies have been constructed or are planned [4]. A partial list of current and past projects related to space-

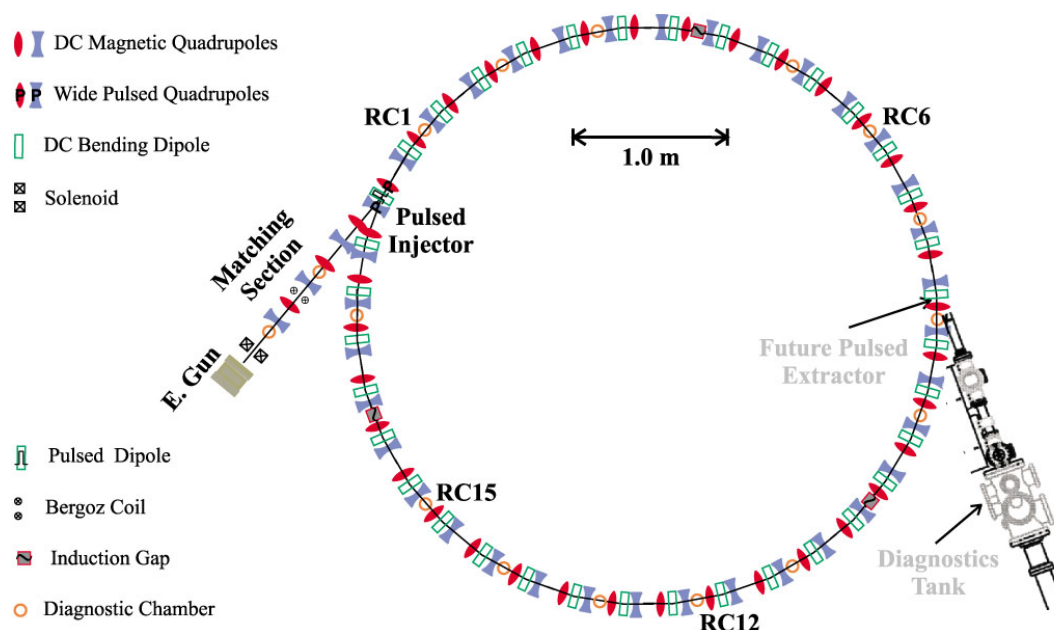


Figure 1: Current Layout of UMER. The Steering elements and Helmholtz coils are not shown. The earth's field points at an angle of 67° relative to the vertical into the plane of the ring.

charge physics include the small ion-ring at Livermore National Laboratory, the Small Isochronous Ring (SIR) at Michigan State University, the compact ion storage rings used to explore the possibility of “crystalline” beams, and the planned electron model machines for muon and proton Fixed-Field-Alternating-Gradient (FFAG) circular accelerators. Finally, a Paul-trap experiment (PTX) at Princeton Plasma Physics Laboratory is being used for simulation of alternating-gradient transport of intense beams.

The high density of magnets in UMER makes possible the confinement of beams from low to high current without changing external focusing in the periodic lattice (i.e., without changing the operating bare tunes). However, the magnets used have gradient profiles that are “all-edges”, thus requiring special modeling for basic calculations such as envelope matching. In addition, the earth's field introduces a complication for closed orbit distortion calculations and beam steering and control. We discuss in the next section the basic UMER layout and operation, including a brief review of beam steering. In Section III, we describe beam transport over one turn and give examples of some novel diagnostics. In Section IV, we present preliminary results of multi-turn operation with emittance-dominated as well as space-charge dominated beams, and conclude in Section V with a summary of our short and long-term plans for research in UMER.

UMER LAYOUT AND OPERATION

Figure 1 shows the schematics of UMER. The 1.4m-long matching line consists of a short solenoid, 6 quadrupoles, 5 horizontal/vertical magnetic steerers, and Helmholtz coils; the injection section that follows comprises two large

aperture magnetic quadrupoles, a pulsed air-core injection dipole, and two steering elements. The main lattice consists of eighteen sections, each containing 2 FODO cells of air-core magnetic quadrupoles and two bending dipoles. The bending dipoles lie at the vertices of a 36-sided polygon inscribed in an 11.52-m circumference. All but four sections house diagnostics chambers; the diagnostics inside each of these chambers consist of a fast capacitive BPM and a fluorescent screen. Three of the ring sections contain glass adapters intended for induction modules currently under development.

The electron energy is 10 keV, and the pulse duration is 20-100 nS, with a 60 Hz repetition rate. Since the energy is so low, the earth's magnetic field is a major factor; in fact, we rely on its action for about one third of bending in the ring. However, we compensate for the earth's field over the straight matching section by means of Helmholtz coils, and also compensate, approximately, for the horizontal component of the field in each ring section. The latter helps us to minimize undesired vertical centroid oscillations.

As mentioned in the introduction, the high density of quadrupoles in the UMER lattice allows us to transport all beam currents without changing the bare tune. This can be seen from the following approximate equation for the average beam radius in a uniform-focusing approximation of the lattice [1]:

$$a = \frac{S}{\sigma_0} \left(\epsilon \frac{\sigma_0}{S} + K \right)^{1/2}, \quad (2)$$

where $S=0.32$ m is the full-lattice period, σ_0 is the “zero-current” phase advance per period (72.9° , nominal), ϵ is the 4rms, unnormalized emittance, and K is the beam perveance (proportional to beam current). The beam ra-

radius a is proportional to $S^{1/2}$ in the regime of emittance-dominated transport, and to S in the limit of strong space charge. Thus, having closely spaced focusing elements is more efficient for the transport of intense beams, other parameters being equal, than for the transport of low current.

The experiments underway in UMER utilize the first three beam currents tabulated above. All three currents are obtained through collimation of the full beam (100 mA, 10 keV) with apertures on a rotatable plate near the electron gun exit. Further, an effort is made to operate the triode gun under the same conditions (anode-cathode gap and grid bias voltage) for all three currents and in such a way that no visible halos occur before injection. Since UMER is intended for space-charge dominated beam transport, its operation has been optimized at the commissioning stage with space-charge dominated beams. However, operation with low current is now being emphasized for understanding the basic problems underlying beam steering for closed orbit and multi-turn operation.

The first problem in UMER is to define a reference or design trajectory. Following the standard definition, the reference trajectory would be determined by the action of bending dipoles and the earth's B-field on a single particle with zero injection errors (including energy). The net horizontal deflection from the action of the earth's B-field (vertical component) is 79.2° , while the combined bending from the main dipoles is 280.8° . But the earth's field acts everywhere while the dipoles have an effective length of only 3.76 cm. Thus, if the ambient B-field were perfectly uniform around the ring, and there were no mechanical errors, each dipole would have to be powered with the same current (2.35 A), 22% lower, approximately, than the required current (3.0 A) if the earth's field were shielded. In reality, because of the non-uniformity of the ambient field and unavoidable mechanical imperfections, the dipoles must be set individually to achieve suitable centroid orbits.

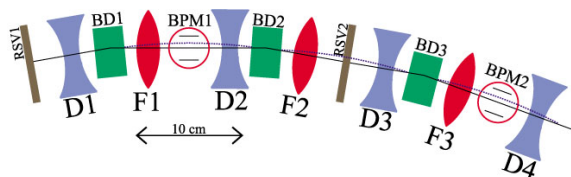


Figure 2: Pictorial representation of centroid motion in UMER sections. Without the earth's B-field, the reference trajectory in the *horizontal* plane is as indicated by the solid line. The actual beam centroid trajectory is close to the dotted line shown, with a radial offset of the order of 1 mm (exaggerated in the diagram) midway between bending dipoles.

In practice, beam steering around the ring is done in this way: the bending dipole (BD1 in Figure 2) upstream of the two quadrupoles (F1 and D2 in Fig. 2) on both sides of a diagnostic chamber (BPM1) is adjusted to minimize the horizontal beam offsets through the quadrupoles.

For the procedure, the quadrupole currents are scanned around the nominal values while the beam's horizontal position is monitored at the next ring chamber (BPM2 in Fig. 2). Thus, the beam steering algorithms aim at minimizing (in a least-square sense) the horizontal beam centroid offsets through the quadrupoles. However, because of the earth's field, the trajectories between bending dipoles are not straight, causing a radial offset of the order of 1 mm relative to the BPM axis at the location of the ring chambers. The beam centroid zigzags between bending dipoles and crosses the quadrupoles off axis so, even in the ideal situation of perfectly-aligned quadrupoles, the beam is slightly deflected towards the pipe axis by the focusing quadrupoles (F1-F3) and in the outward radial direction by the defocusing ones (D2-D4). Under these conditions, the optimal reference orbit is one with a small offset through the quadrupoles.

As mentioned before, the horizontal component of the earth's B-field is compensated by means of coils installed over each ring section. The currents through these coils are individually set based on carefully-measured B-field values around the ring. Further vertical steering corrections are done with short dipoles located midway between ring sections (RSV1 and RSV2 in Fig. 2).

More systematic beam steering can be based on the sensitivity matrix constructed by studying beam deflection in all 14 BPMs for small current changes in all correctors (bending dipoles for horizontal steering, and short vertical dipoles for vertical corrections). Ultimately, all 72 quadrupoles, including those in the injector, can be used as "virtual BPMs" to enlarge the sensitivity matrix. Approximate inversion of the matrix through standard single-value-decomposition (SVD) techniques then yields the information for ideal steering for closed orbit conditions. Additional details of the procedure and progress for first-turn steering can be found in [5].

FIRST-TURN EXPERIMENTS AND NEW DIAGNOSTICS

Before the ring lattice was completed, transport experiments were conducted with a simplified DC version of the injector [6]. Beam steering, envelope matching and skew quadrupole corrections were studied for a number of beam currents, similar to those tabulated above [7]. Further, halos were observed whose origin was traced, based on computer simulations, to a combination of factors: initial particle distribution, residual mismatch and skew quadrupole errors [8]. To conclude this stage of the project with DC injection, an experiment with highly asymmetric focusing ($\nu_{0x}=5.72$, $\nu_{0y}=7.34$) of a space-charge dominated beam (10 keV, 7.2 mA) revealed halos noticeably different from those occurring with symmetric focusing [9].

Figure 3 illustrates three examples of RMS envelope matching with the old injector lattice which consisted of a short solenoid, seven quadrupoles and a bending dipole, all DC powered. Details of the calculations and additional

examples are given in Ref. [10]. Matching calculations for the pulsed injector now in use are more involved but lead to very similar envelopes.

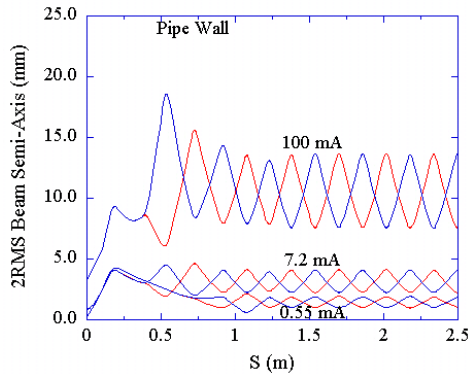


Figure 3: Examples of envelope matching in UMER for three beam currents at 10 keV, $\nu_0=7.29$. The lattice geometry corresponds to DC injection [10]. Only the 0.55 mA beam is emittance dominated.

The experiments underway with the new injector (next section) rely on a good first-turn base line for injection, beam steering and envelope matching. Thus, detailed beam measurements over the first turn are especially important for achieving multi-turn transport. Examples of beam diagnostics and techniques under development for UMER are tomography and optical transition radiation (OTR).

Emittance measurements through quadrupole scans and/or pepperpot techniques were standard in early tests before the ring was closed. However, it is desirable to know the details of beam phase space near the source and over the first turn. Since pepperpots cannot be easily implemented in UMER without an extraction section, alternative techniques are required. Beam tomography, introduced some years ago, represents an interesting alternative for phase-space mapping; it is based on quadrupole scans and beam profiling. In time-resolved tomography, for example, 6D phase space is determined from beam-profile data obtained with ultra-fast sensors and cameras [11]. In UMER, we have pioneered the (time-integrated) tomography of space-charge dominated beams [12]. Currently, we are using tomography in experiments and particle-in-cell simulations (with the WARP code), to explore the validity of this technique, which is based on linear beam transformations, to space-charge dominated beams [13] and, in particular, to first-turn analysis of the UMER.

MULTI-TURN EXPERIMENTS

The new injector (see Fig. 1) comprises a number of pulsed elements and timing electronics that require careful tuning to recover the first-turn baseline of the DC injection experiments. In one scheme, the beam is injected with a horizontal offset through a defocusing (in the horizontal plane) wide-aperture quadrupole near the intersection of

the matching section and the ring. Ideally, the small bending by the quadrupole (about 2^0-3^0), plus steering from correcting elements, brings the beam to the center of the injection dipole, which deflects the beam on-axis through a second large-aperture quadrupole and into the ring. The polarity of the injection dipole is then inverted before the beam completes one turn in 197 ns, and in order to store the beam, the polarity swing is made asymmetrical because of the opposite actions of the earth's B-field during injection and circulation. In a second scheme under testing, designed after a Collins insertion, the two large aperture quadrupoles are powered off, so extra current has to be applied to the injection dipole and a completely different rms-envelope matching has to be implemented. Other schemes are possible where the earth's B-field is shielded over the entire ring, or just over the injection section.

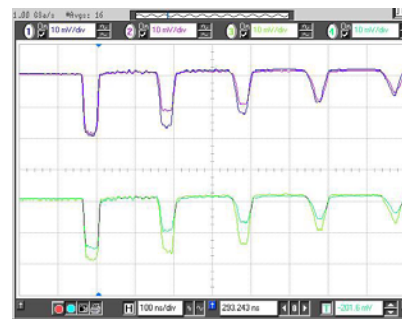


Figure 4: BPM signals from chamber RC1 for multi-turn operation in UMER with strong space-charge (10 keV, 20 mA, 50 ns.) The top (bottom) signals represent the horizontal (vertical) BPM channels. Current was detected for over 10 turns. See text for discussion.

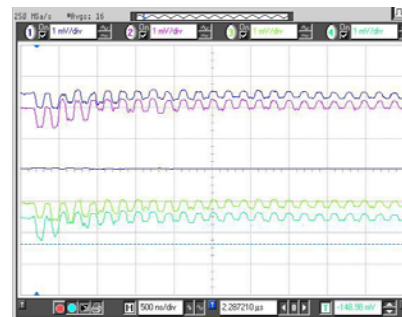


Figure 5: BPM signals from chamber RC2 for multi-turn operation in UMER with low current (10 keV, 600 μ A, 100 ns.) The top (bottom) signals represent the horizontal (vertical) BPM channels. Current was detected for over 100 turns. See text for discussion.

Figure 4 shows an example of our first results of multi-turn operation with a (initial) strongly space-charge dominated beam: 10 keV, 20 mA (approx.) injected current, 50 ns pulse length. Although beam loss is obvious, significant current was detected after at least 10 turns. Also clearly seen in Fig. 4 is the erosion of the beam edges,

which is not as strong with a 100 ns beam pulse. Whether the beam losses are caused by simple scraping due to large centroid oscillations, or mostly by halo formation, or resonance issues is not clear at the time of writing. Errors in injection, beam steering for closed orbit conditions, and residual envelope mismatch may all contribute to current loss. Additional work with timing for re-circulation and skew quadrupole corrections may also be required. Despite these shortcomings, multi-turn operation of such high current beam is a significant result: calculations indicate that even for the surviving beam (after 9 turns), the corresponding tune shift amply exceeds the Laslett tune shift of 0.25.

Multi-turn operation with an emittance-dominated beam was also achieved, as illustrated in the oscilloscope screen of Figure 5. Beam loss appears to occur after the second or third turn, but the low current beam survives with half the injected current and no further losses for another 25 turns, approximately. Current can be detected for over 100 turns. Furthermore, the calculated tune shift is also larger than 0.25. No beam-edge erosion is evident, although the time resolution (sampling) may not be sufficient in this case to discern changes.

Tables 2 and 3 summarize early estimates of the intensity parameter, tune depression and tune shift based on first measurements of multiturns in UMER.

Table 2: Parameters for multi-turn with strong space charge at 10 keV, bare tune $\nu_0 = 7.29$.

	Beam Current	Emitt. (μm)	χ , ν/ν_0	$\Delta\nu$
Injected	18.6 mA	24	0.70, 0.55	3.3
After 9 turns	3.6 mA	10-25	0.48-0.24, 0.72-0.87	2.0-0.9

Table 3: Parameters for multi-turn with emittance-dominated beam at 10 keV, bare tune $\nu_0 = 7.29$.

	Beam Current	Emitt. (μm)	χ , ν/ν_0	$\Delta\nu$
Injected	690 μA	5.6	0.20, 0.89	0.80
After 25 turns	300 μA	4.6	0.12, 0.94,	0.45

SUMMARY AND FUTURE WORK

The University of Maryland Electron Ring is a platform for scaled experiments and code benchmarking in beam physics. The ring is designed for beam transport over a broad range of intensities, but in all cases space charge is a significant factor. Multi-turn operation of both emittance-dominated and (initially) space-charge dominated beams

was achieved very recently. Despite the occurrence of beam losses, especially in the latter case, the results are significant because the estimated space-charge tune shifts (Laslett's tune shift) amply exceed the traditional limit of 0.25 for circular machines.

Short-term plans include: a full stability analysis of the ring, detailed tune measurements with improved diagnostics and signal processing, optimized first-turn transport (steering, envelope matching and skew corrections), improved steering for closed orbit and multi-turn, experiments and simulations for resonance crossings, and experiments with density and current perturbations (with photoemission and otherwise).

Medium to long-term plans include: experimental study of energy spread evolution, experiments with anisotropic beams in search of coupling resonances (Montague), emittance exchange and equipartitioning; beam extraction, detailed PIC simulations for multi-turn, and development of modules for acceleration to 50-80 keV.

REFERENCES

- [1] M. Reiser, *Theory and Design of Charged-Particle Beams* (Wiley & Son, New York, 1994).
- [2] M. Reiser *et al.*, Proc. 1999 Part. Accel. Conf., New York, NY (IEEE, New York, 1999), p. 234; Ronald C. Davidson and Hong Qin, *Physics of Intense Charged Particle Beams in High Energy Accelerators*, World Scientific, Singapore (2001), p. 8.
- [3] G. Danby, E. Gill, J. Keane and A. W. Maschke, BNL Report 50643, March 1977 (Brookhaven National Laboratory).
- [4] L. Ahle *et al.*, Nucl. Instrum. Phys. Res. A **464**, 557-562 (2001); E. Pozdeyev *et al.*, in Proc. 2005 Part. Accel. Conf., Knoxville, TN, p. 159; Y. Yuri and H. Okamoto, Phys. Rev. ST Accel. Beams, **8** 114201 (2005); S.R. Koscielniak and C. Johnstone, in Proc. of the 2005 Part. Accel. Conf., Knoxville, TN, p. 3173; E.P. Gilson *et al.*, Phys. Rev. Lett., **92**, 155002 (2004).
- [5] M. Walter *et al.*, Phys. of Plasmas, **13**, 056703 (2006).
- [6] S. Bernal *et al.*, Proc. 2005 Part. Accel. Conf., Knoxville, TN (IEEE, New York, 2005), p. 469.
- [7] Hui Li *et al.*, Nucl. Instr. and Meth. Phys. Res. A, **544**, 367 (2005).
- [8] R.A. Kishek *et al.*, Proc. 29th ICFA Advanced Beam Dynamics Workshop on Beam Halo Dynamics, Diagnostics, and Collimation, Montauk, NY, May 2003, AIP, New York (2003), p. 89.
- [9] S. Bernal *et al.*, in Proc. 2005 Part. Accel. Conf., Knoxville, TN (IEEE, New York, 2005), p. 892.
- [10] S. Bernal *et al.*, Phys. Rev. ST Accel. Beams, **9**, 064202 (2006).
- [11] V. Yakimenko, M. Babzien, I. Ben-Zvi, R. Malone, and X.-J. Wang, Phys. Rev. ST Accel. Beams, **6** 122801 (2005)
- [12] H. Li, Ph.D. Thesis, Department of Electrical Engineering, University of Maryland, College Park, 2004.
- [13] D. Stratakis *et al.*, submitted to Phys. Rev. ST Accel. Beams.